11th International Symposium on Systems with Fast Ionic Transport, ISSFIT 11

Synthesis and testing of BCZY/LNZ mixed proton–electron conducting composites for fuel cell applications

K. Zagórski[a]*, T. Miruszewski[a], D. Szymczewska[b], P. Jasinski[b], M. Gazda[a]

[a] *Faculty of Applied Physics and Mathematics, Gdansk University of Technology, ul. Narutowicza 11/12, Gdansk 80-233, Poland*
[b] *Faculty of Electronics, Telecommunication and Informatics, Gdansk University of Technology, ul. Narutowicza 11/12, Gdansk 80-233, Poland*

Abstract

A composite of $BaCe_{0.6}Zr_{0.2}Y_{0.2}O_{3-\delta}$ and Li_2O:NiO:ZnO was investigated for fuel cell applications. The composite was successfully synthesized and its phase stability was confirmed at temperatures up to 900°C. The influence of sintering and pressing aids on density was also investigated. Electrical properties were measured. DC electrical conductivity was about $8 \cdot 10^{-4}$ S/m at 845 K. Open circuit voltage measurements in wet hydrogen have shown that the composite can be used in single layer fuel cells.

Keywords: Barium cerate; barium zirconate; composite; proton conductor; semiconductor; fuel cell

1. Introduction

Conventional state of the art solid oxide fuel cells are composed of three layers: cathode, anode and electrolyte. The electrolyte layer is especially important because, in order to maximize the fuel cell efficiency, the electrolyte must be as thin as possible (<<100μm) and simultaneously impermeable [1]. These requirements significantly increase manufacturing costs of SOFCs, which are one of the biggest challenges for their industrial commercialization.

* Corresponding author. Tel.: +48-58-348-66-12.
  E-mail address: kzagorski@mif.pg.gda.pl

The recent concept of an electrolyte–less single layer fuel cell device presented by Zhu et al. has gathered a lot of attention in the fuel cell community [1, 2]. In this device the single layer is a homogenous composite of an ion conducting ceramic and metal oxide semiconductors [2]. While the overall electrochemical reaction is the same as in a conventional fuel cell, the lack of electrolyte – a blocking layer for electrons – implies a different working principle of charge separation in the single layer device.

The ion conducting material provides a percolating path for ions whereas the metal oxide semiconducting material is thought to both provide a percolating path for electrons and form n–p junctions. Together, these materials form a device that performs fuel cell functions by combining electrochemical and physical principles. During cell operation, that is, when hydrogen and oxygen are provided, low and high pO_2 lead to forming n- and p-type conducting regions. As a result of hydrogen and oxygen dissociation on the surfaces of n– and p–type regions they gain charges but the junctions between them are depleted of charge. With such a polarization of the junctions, the semiconducting phase displays a diode effect and conducts electrons only in one direction while ionic transport is unaffected. Therefore, a short circuit is avoided and a cell potential may be generated and collected [4].

In the case of the devices constructed and studied by Zhu et al. samarium substituted ceria was used as an ionic conductor. Oxides, which were used as either p– or n–type semiconductors, were for instance: Li–doped NiO and ZnO [2] or MgO [3]. NiO is a p–type conductor and its conductivity is enhanced by Li_2O doping [5]. ZnO is usually a n–type conductor, but can also exhibit p–type conductivity in certain conditions [6]. Additionally, NiO and ZnO have been reported to conduct both protons and oxygen ions [7, 8, 9, 10]. It should be stressed that so far, the details of phenomena occurring in a single layer cell has been neither fully researched nor understood. While potentially groundbreaking, the concept thus far has not been confirmed by any other group. If the concept was positively verified, one of the possible ways of further improving the single layer device would be lowering its operational temperature by substituting the oxide ion conductor with a proton conductor.

There are two major concerns with this kind of composite. Firstly, high reactivity of the constituent phases with respect to each other could lead to formation of secondary phases with a detrimental influence on key properties of the composite. To avoid such an outcome, it is necessary to establish the composite highest synthesis temperature. The second concern is sufficient mechanical robustness required for an efficient manufacturing process and stable fuel cell operation. In order to achieve that, the powders should be easily pressable into pellets without visible flaws and reach a sufficient density during sintering. To promote the formation of dense ceramics surfactants and pressing aids such as stearic acid [15] and polivynyl alcohol [14] or densification aids such as alkali carbonates [12] can be added to the powder before pressing and sintering.

In this work, a composite of proton conducting $BaCe_{0.6}Zr_{0.2}Y_{0.2}O_{3-\delta}$ and $Li_2O{:}NiO{:}ZnO$ oxides was synthesized. The stability of constituent phases, influence of additives on densification as well as the composite applicability for fuel cell systems were investigated.

Nomenclature

BCZY $BaCe_{0.6}Zr_{0.2}Y_{0.2}O_{3-\delta}$
LNZ $Li_2O{:}NiO{:}ZnO$ (0.15:0.45:0.4)
PVA $[CH_2CH(OH)]_n$ Polyvinyl alcohol
STEA $CH_3(CH_2)_{16}CO_2H$ Stearic acid
LNC $(Li–0.5Na)_2CO_3$

---

2. Experimental

The $BaCe_{0.6}Zr_{0.2}Y_{0.2}O_{3-\delta}$ (BCZY) proton conductor was prepared by solid state synthesis. Stoichiometric amounts of $BaCO_3$, CeO_2, $ZrOCl_2$ x $8H_2O$ and Y_2O_3 powders were ball milled for 24 h. After milling the powder was dried, pressed uniaxially with a load of 440 MPa and sintered at 1500°C for 24 h.

The $Li_2O{:}NiO{:}ZnO$ (LNZ) semiconducting oxides were prepared by solid state synthesis. Stoichiometric amounts of ZnO, $LiCO_3$ and $Ni(NO_3)_2$x$6H_2O$ powders were mixed, ground in an agate mortar and sintered at 800°C for 2

hours. Resultant BCZY and LNZ powders were mixed in a 2:1 weight ratio and ground in an agate mortar to get a homogenous mixture. Using the resultant powder mixture, three kinds of samples were prepared:

- BCZY/LNZ control samples with no additives
- BCZY/LNZ with an addition of 3% wt. polivynyl alcohol and 3% wt. stearic acid (BCZY/LNZ/PVA/STEA)
- BCZY/LNZ with 5% wt. $(Li–0.5Na)_2CO_3$ (BCZY/LNZ/LNC)

The BCZY/LNZ/PS and BCZY/LNZ/LNC powders were prepared by adding the appropriate amounts of PVA, STEA and LNC and subsequent ball milling in isopropanol for 24 h. The slurries were dried in an oven at 85°C for 24 hours. All powders were pressed uniaxially into pellets approximately 1 mm thick. Both BCZY/LNZ/PVA/STEA and BCZY/LNZ/LNC powders form pellets of superior quality, when compared with pure BCZY/LNZ. The BCZY/LNZ pellets were sintered repeatedly at increasing temperatures: 700, 900 and 1000°C for 2 hours. Samples with PVA/STEA, LNC and pure BCZY/LNZ were sintered at 900°C for 24 hours.

The densities of sintered samples were measured using the Archimedes method and compared with the calculated theoretical densities [11, 12]. XRD data on BCZY, LNZ and the BCZY/LNZ composite was collected by a Philips X"Pert Pro diffractometer. Micrographs of BCZY/LNZ, BCZY/LNZ/PVA and BCZY/LNZ/LNC composite samples, both as sintered and treated in wet H_2, were captured using a Phenom G2 PRO scanning electron microscope.

Applicability of the BCZY/LNZ composite for fuel cell use was evaluated in the 473−873 K temperature range by OCV measurement in wet H_2 using an in–house testing cell [16]. Silver paste was painted onto each side of the pellets to act as electrodes and current collectors. An ambient air (supplied by pump) and wet hydrogen were used as an oxidant and a fuel, respectively. Three different flow rates of hydrogen were used: 100, 300 and 600 ml per minute. Temperature dependence of electrical conductivity of BCZY/LNZ and BCZY/LNZ/LNC was measured in air in the 645–845 K temperature range using a four–probe DC setup.

3. Results and discussion

Results of density measurements are shown in Table 1. The theoretical density of BCZY/LNZ was calculated to be 5.99 g/cm^3 [11]. The theoretical density of BCZY/LNZ/PVA/STEA is also 5.99 g/cm^3 due to decomposition of the additives during sintering. The density of BCZY/LNZ/LNC was calculated to be 5.92 g/cm^3 [12].

It was found that repetitive sintering steps result in a slight increase in density, while a long single step sintering has no influence on density. While the BCZY/LNZ/PVA/STEA sample result indicates that adding PVA and stearic acid does not affect density, it does enhance pellet formation. The BCZY/LNZ/LNC sample shows a substantial increase in density, which results in the increased robustness of the pellets and ease of handling.

Table 1. Densities of the composites prepared in different conditions.

Sample	Temperature [°C]	Sintering time [h]	Density [%]
BCZY/LNZ	700	2	65
BCZY/LNZ	700 and 900	2 +2	67
BCZY/LNZ	700, 900 and 1000	2+2+2	69
BCZY/LNZ	900	24	64
BCZY/LNZ/PVA/STEA	900	24	64
BCZY/LNZ/LNC	900	24	77

The results of XRD analysis are shown in Figs. 1 and 2. The patterns of Li_2O:NiO:ZnO, $BaCe0.6Zr0.2Y0.2O3–\delta$ and the BCYZ/LNZ composite sintered at 900°C are shown in Fig. 1. Figure 2 shows the XRD patterns of the composite sintered at different temperatures. It can be seen that BCYZ/LNZ composite constituent phases are stable in temperatures up to 900°C. In the BCZY/LNZ composite XRD pattern peaks corresponding to the BCZY phase

are prevalent, the LNZ phase peaks are comparatively less intensive but still distinguishable. Figure 2 shows how the XRD pattern changes with synthesis temperature increasing from 700 to 1000°C. With increasing temperature the distance between peaks corresponding to ZnO and NiO (LNZ phase) is decreasing. At 1000°C the peaks begin to overlap. The peak shift is caused by a change in lattice constant This indicates diffusion between ZnO and NiO, and formation of a solid solution of ZnO in NiO. Such a process of NiO–ZnO solid solution formation at temperatures above 600°C was already reported [6].
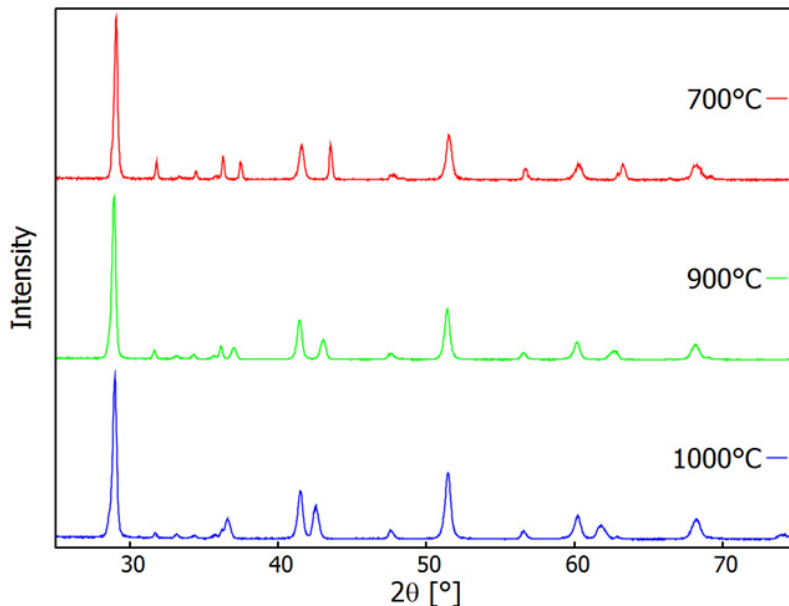

Fig. 1 XRD patterns of the BCYZ/LNZ composite (sintered at 900°C), BCZY (1500°C) and LNZ (800°C); collected at room temperature.
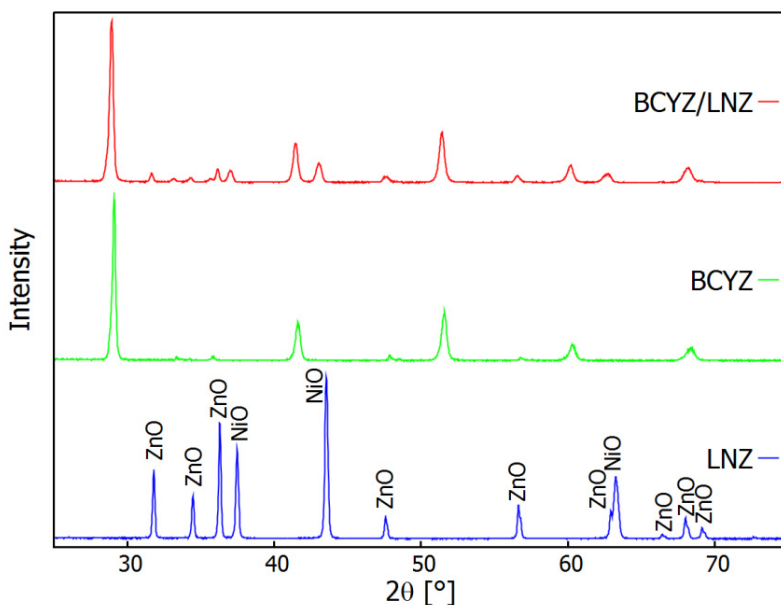

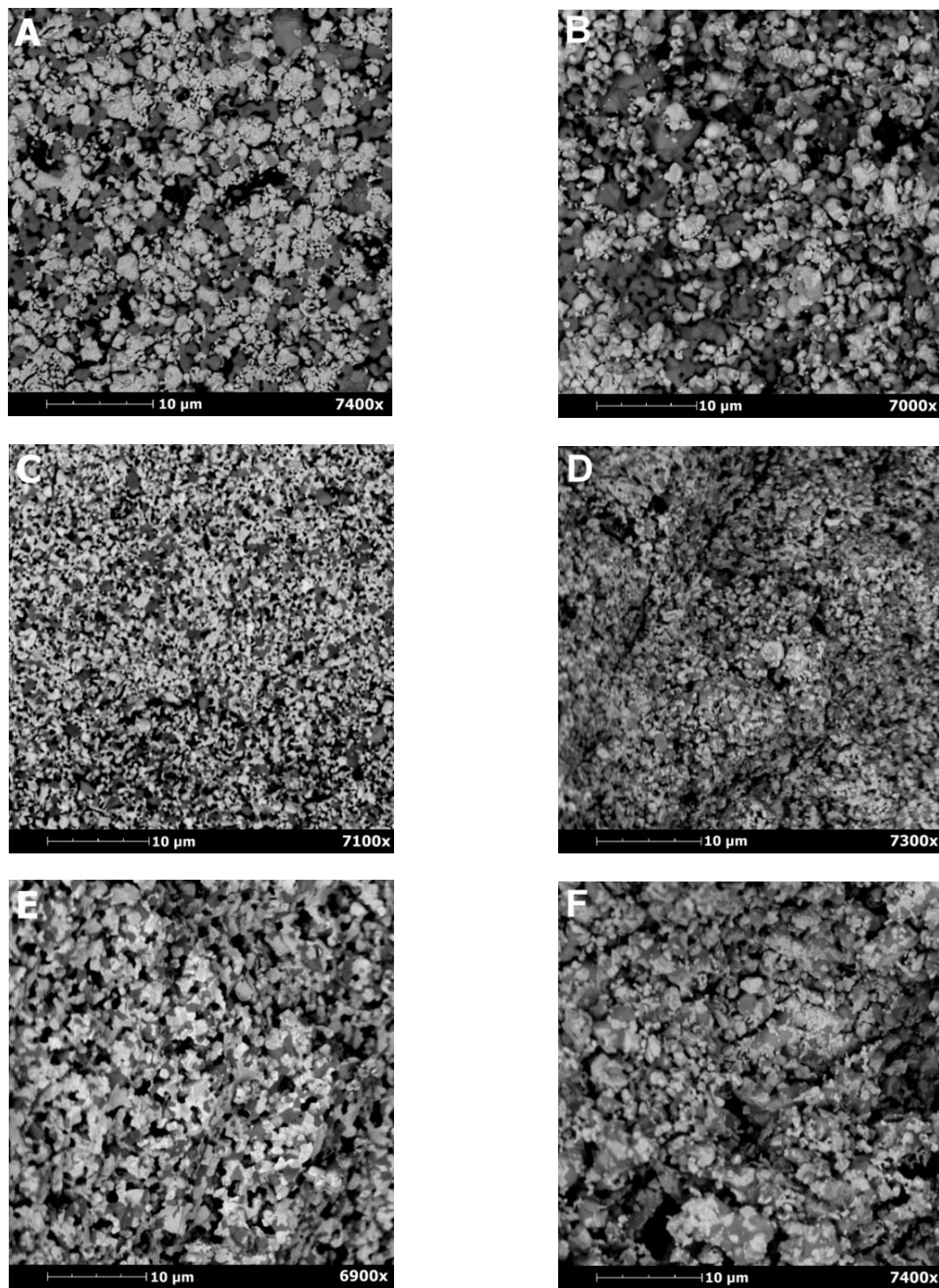Fig. 2 XRD patterns of the BCYZ/LNZ composite sintered at increasing temperature.

Fig. 3 SEM micrographs. Scale is 10μm. A) BCZY/LNZ (as sintered). B) BCZY/LNZ (wet H_2). C) BCZY/LNZ/PVA/STEA (as sintered). D) BCZY/LNZ/PVA/STEA (wet H_2). E) BCZY/LNZ/LNC (as sintered). F) BCZY/LNZ/LNC (wet H_2)

Figure 4 shows that the addition of LNC does not change the BCZY/LNZ XRD pattern, which indicates that the addition of 5% LNC has no influence on the phase composition. Similarly, PVA/STEA has no influence on the phase composition because both additives are organic and decompose below the synthesis temperature.

SEM micrographs of the studied samples are show in Figs. 3A-F. Figure 3A shows the microstructure of as sintered BCZY/LNZ. The BCZY and LNZ phases are mixed homogenously, grains are spheroidal with an average size of 3 μm. Figure 3C shows the microstructure of as sintered BCZY/LNZ/PVA/STEA. Despite no significant difference between densities of the BCZY/LNZ and BCZY/LNZ/PVA/STEA samples, their microstructures substantially differ. Grains are not spheroidal and their average size is significantly smaller, on average 1-1.5 µm. Figure 3E shows the microstructure of as sintered BCZY/LNZ/LNC. The grains have sharp edges and an average size of 2 µm. The microstructures of the samples after the OCV measurements are shown in Figs. 3B, 3D and 3F. It can be seen that average grain size is not influenced by the applied measurement conditions but the grains of BCYZ and LNZ compounds seem to agglomerate together, what is most clearly seen in Fig. 3F and 3D. This may be caused by a local temperature increase which may originate from a direct reaction between oxygen and hydrogen enabled by too high open porosity of the samples.
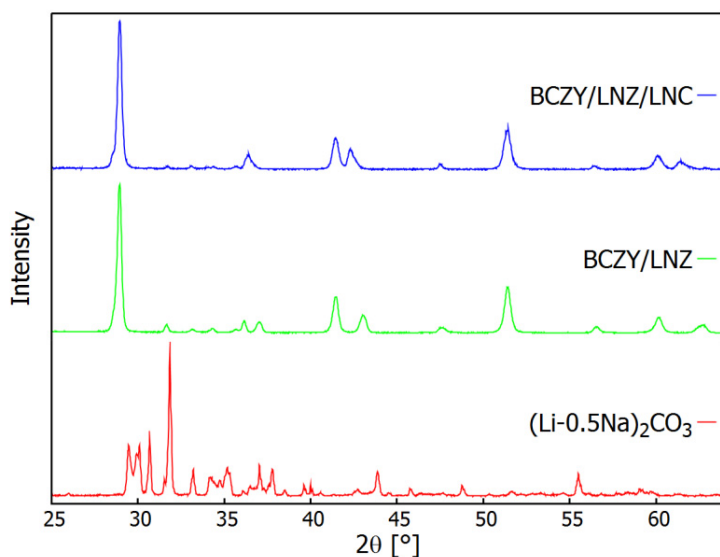

Fig. 4 XRD patterns of the BCYZ/LNZ/LNC composite (sintered at 900°C), BCZY/LNZ (900°C) and $(Li-0.5Na)_2CO_3$ (670°C); patterns collected at room temperature.

The open circuit voltage for pure BCZY/LNZ was measured in the 473–873 K temperature range. For all temperatures, the OCV values for BCZY/LNZ were the order of 10^{-3} V. For BCZY/LNZ/LNC and BCZY/LNZ/PVA/STEA the OCV reached a peak value of 0.26 V and 0.32 V at 873 K, respectively. This indicates that a galvanic cell is formed. In both cases, the OCV was unstable and fluctuated between 0.4 and 0.1 V. The values reported by Zhu. et al. for similar composites but composed of a semiconducting and oxygen conducting materials are around 1 V [1, 4]. Similar values may be expected for proton conducting composites. The voltage fluctuations might be caused by open porosity, which may lead to a direct reaction between oxygen and hydrogen. Taking into account both, the SEM micrographs from Figures 4A-4F and OCV results discussed above, the very low OCV for BCZY/LNZ was most probably caused by its microstructure. This sample in contrast to BCZY/LNZ/LNC and BCZY/LNZ/PVA/STEA was not ball milled during the powder preparation step. This step provided improved homogeneity and decreased grain size for BCZY/LNZ/PVA/STEA and BCZY/LNZ/LNC. We suggest that the ball milling improved the percolation of the semiconducting and proton conduction phases, which in turn caused the increase of open circuit voltage by two orders of magnitude.
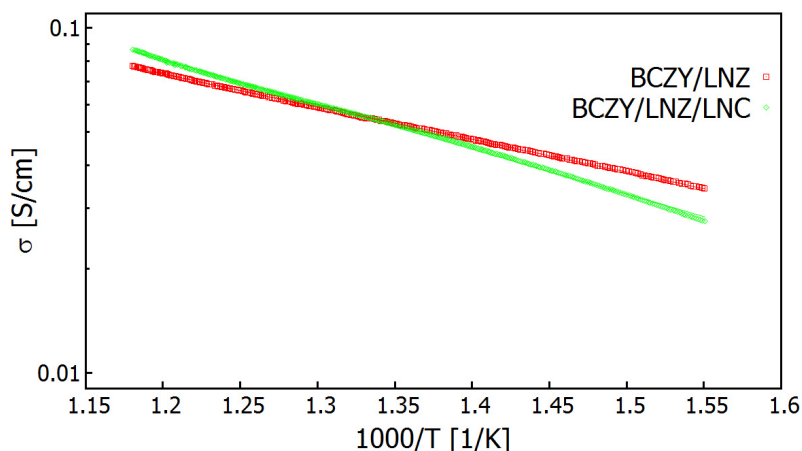
Fig. 5 Conductivity (4-point DC) of BCZY/LNZ and BCZY/LNZ/LNC as a function of temperature.

The DC conductivity temperature dependence of the BCZY/LNZ and BCZY/LNZ/LNC composites sintered at 900°C is presented in figure. 5. It can be seen in figure 5 that the conductivities of both materials are of the same order of magnitude. For example, electrical conductivity for BCZY/LNZ and BCZY/LNZ/LNC at 845 K was $7.78 \cdot 10^{-4}$ S/m and $8.67 \cdot 10^{-4}$ S/m, respectively. The conductivity values and type of temperature dependence of conductivity are typical of semiconductor materials, an expected contribution of the electronically conducting LNZ phase. The conductivity values are higher than those reported in literature for bulk ZnO at 845 K – $0.4 \cdot 10^{-4}$ S/m [17]; but lower than the value of 100 S/m at 845 K reported for bulk Li doped NiO [5]. Since the semiconducting phase studied in this work is a composite of both materials, it seems plausible that its conductivity achieves intermediate values. The calculated values of activation energy of conductivity for BCZY/LNZ and BCZY/LNZ/LNC are 0.2 eV and 0.3 eV, respectively. The higher activation energy of conductivity resulting from the addition of LNC to the BCZY/LNZ composite might be attributed to the presence of the electronically insulating carbonate phase.

4. Conclusions

These results show that a single layer fuel cell concept, like the one presented by Zhu et al., is feasible when using a proton conducting phase instead of an oxygen ion conducting phase. The highest OCV was 0.325 V for the BCZY/LNZ/PVA/STEA samples. Possible further avenues of research, aimed at increasing the OCV and stability of the device, are adjusting porosity, utilizing nanostructured BCZY and LNZ in varying compositions as well as other proton and semiconducting materials and systems.

References

[1] B. Zhu, R. Raza, G. Abbas, M. Singh. An Electrolyte-Free Fuel Cell Constructed from One Homogenous Layer with Mixed Conductivity. *Adv. Funct. Mater.* 2011; 21: 2465–2469.
[2] L. Fan, C. Wang, M. Chen, B. Zhu. Recent development of ceria-based (nano)composite materials for low temperature ceramic fuel cells and electrolyte-free fuel cells. *J. Power Sources* 2013; 234: 154–174.
[3] H. Hua, Q. Lina, Z. Zhua, X. Liub, B. Zhu. Time-dependent performance change of single layer fuel cell with $Li_{0.4}Mg_{0.3}Zn_{0.3}O/Ce_{0.8}Sm_{0.2O2-\delta}$ composite. *Int. J. Hydrogen Energy* 2014; 39:10718–10723.
[4] B. Zhu, R. Raza, Q. Liu, H. Qin, Z. Zhu, L. Fan, M. Singha, P. Lund. A new energy conversion technology joining electrochemical and physical principles. *RSC Adv.* 2012; 2:5066–5070.

[5] H. P. Rooksgyi, M. W. Vernon. Lithium– and Galium–doped nickel oxide. *Brit. J. Appl. Phys*. 1966; 17: 1227–1228.

[6] Ü. Özgür, Y. Alivov, C. Liu, A. Teke, M. A. Reshchikov, S. Doğan, V. Avrutin, S-J. Cho and H. Morkoç. A comprehensive review of ZnO materials and devices. *J. Appl. Phys.*, 2005; 98: 041301–041403.

[7] D. Michael, D. B. Buchholz, W. H. Alexander and P. H. C. Robert. p-Type semiconducting nickel oxide as an efficiency-enhancing anode interfacial layer in polymer bulk-heterojunction solar cell. *Proc. Natl. Acad. Sci. U. S. A.* 2008; 8: 2783–2787.

[8] L. Chen, L. Li and G. Li. Surface hydration-mediated conduction of NiO nanocrystals. *Solid State Ionics* 2008; 179: 712–717.

[9] C. Dubois, C. Monty, J. Philibert. Influence of oxygen pressure on oxygen self-diffusion in NiO. *Solid State Ionics*. 1984; 12: 75–78.

[10] J. Carrasco, N. Lopez, and F. Illas. First Principles Analysis of the Stability and Diffusion of Oxygen Vacancies in Metal Oxides. *Phys. Rev. Lett.* 2004; 93:225502.

[11] P. Sawant, S. Varma, B.N. Wani, S.R. Bharadwaj. Synthesis, stability and conductivity of $BaCe_{0.8–x}Zr_xY_{0.2}O_{3–\delta}$ as electrolyte for proton conducting SOFC. *Int. J. Hydrogen Energy* 2012; 37: 3848–3856.

[12] K.-Y. Park, T.-H. Lee, J.-T. Kim, N. Lee, Y. Seo, S.-J. Song, J.-Y. Park. Highly conductive barium zirconate-based carbonate composite electrolytes for intermediate temperature-protonic ceramic fuel cells. *J. Alloys Compd*. 2014; 585: 103-110.

[13] H. Kedesdy, A. Drukalsky. X-Ray Diffraction Studies of the Solid State Reaction in the NiO-ZnO System. *J. Am. Chem. Soc*. 1954; 76.23: 5941–5946.

[14] M.A. de la Rubia, M. Peiteado, J.F. Fernandez, , A.C. Caballero. Compact shape as a relevant parameter for sintering ZnO–Bi2O3 based varistors. *J. Eur. Ceram. Soc*. 2004; 26: 1209-1212.

[15] W. J. Tseng, D.-M. Liu, C.-K. Hsu. Influence of stearic acid on suspension structure and green microstructure of injection-molded zirconia ceramics. *Ceram. Int*. 1999; 25: 191–195.

[16] K. M. Dunst, J. Karczewski, T. Miruszewski, B. Kusz, M. Gazda, S. Molin, and P. Jasinski. Investigation of functional layers of solid oxide fuel cell anodes for synthetic biogas reforming. *Solid State Ionics*. 2013; 251: 70–77.

[17] P. H. Miller. The Electrical Conductivity of Zinc Oxide. *Physical Review 1941; 60:890-894.*